



biblio.ugent.be

The UGent Institutional Repository is the electronic archiving and dissemination platform for all UGent research publications. Ghent University has implemented a mandate stipulating that all academic publications of UGent researchers should be deposited and archived in this repository. Except for items where current copyright restrictions apply, these papers are available in Open Access.

This item is the archived peer-reviewed author-version of: Fluorescence Correlation Spectroscopy to find the critical balance between extracellular association and intracellular dissociation of mRNA complexes

Authors: Zhang Z., De Smedt S.C., Remaut K.

In: Acta Biomaterialia 75: 358-370

To refer to or to cite this work, please use the citation to the published version:

Zhang Z., De Smedt S.C., Remaut K. (2018) Fluorescence Correlation Spectroscopy to find the critical balance between extracellular association and intracellular dissociation of mRNA complexes

Acta Biomaterialia 78: 1-18

DOI: 10.1016/j.actbio.2018.05.016

Title.

Fluorescence Correlation Spectroscopy to find the critical balance between extracellular association and intracellular dissociation of mRNA-complexes

Author names and affiliations.

Heyang Zhang¹, Stefaan C. De Smedt^{1,2*}, Katrien Remaut^{1*}

¹Laboratory of General Biochemistry and Physical Pharmacy, Faculty of Pharmaceutical Sciences, Ghent University, Ghent 9000, Belgium;

²College of Chemical Engineering, Nanjing Forestry University (NFU), Nanjing 210037, PR China;

Corresponding authors.

Prof. Dr. Katrien Remaut, Prof. Dr. Stefaan C. De Smedt;

Prof. Dr. Katrien Remaut will handle correspondence at all stages of refereeing and publication, also post-publication.

E-mail: Katrien.Remaut@UGent.be; Stefaan.Desmedt@UGent.be

Tel: +32 9 264 80 76, Fax: +32 9 264 81 89

Corresponding address: Ottergemsesteenweg 460, 9000 Gent, Belgium.

Abstract:

Fluorescence Correlation Spectroscopy (FCS) is a promising tool to study interactions on a single molecule level. The diffusion of fluorescent molecules in and out of the excitation volume of a confocal microscope leads to the fluorescence fluctuations that give information on the average number of fluorescent molecules present in the excitation volume and their diffusion coefficients. In this context, we complexed mRNA into lipoplexes and polyplexes and explored the association/dissociation degree of complexes by using gel electrophoresis and FCS. FCS enabled us to measure the association and dissociation degree of mRNA-based complexes both in buffer and protein-rich biological fluids such as human serum and ascitic fluid, which is a clear advantage over gel electrophoresis that was only applicable in protein-free buffer solutions. Furthermore, following the complex stability in buffer and biological fluids by FCS assisted to understand how complex characteristics, such as charge ratio and strength of mRNA binding, correlated to the transfection efficiency. We found that linear polyethyleneimine prevented efficient translation of mRNA, most likely due to a too strong mRNA binding, whereas the lipid based carrier Lipofectamine[®] messengerMAX did succeed in efficient release and subsequent translation of mRNA in the cytoplasm of the cells. Overall, FCS is a reliable tool for the in depth characterization of mRNA complexes and can help us to find the critical balance keeping mRNA bound in complexes in the extracellular environment and efficient intracellular mRNA release leading to protein production.

Keywords: FCS, mRNA complex formation, mRNA delivery, biofluids, complex stability

1. Introduction

Nucleic acids have been explored widely in basic research and biomedical applications in the past decades. There is a growing interest in the use of mRNA as a potential therapeutic in various medical indications, ranging from hereditary or acquired metabolic diseases to regenerative diseases, therapeutic cancer vaccination and protein-replacement [1]. Conceptually, mRNA exerts its function in the cytoplasmic compartment and does not depend on nuclear envelope breakdown. Also, unlike plasmid DNA (pDNA), there is no risk of insertional mutagenesis for mRNA, which provides a substantial safety advantage for clinical practice [2][3][4]. In addition, mRNA production is relatively simple and low-cost as there is no need to select and incorporate a specific promoter into the transfection construct [5].

To advance protein-replacement therapies [1][6][7][8][9][10], efficient mRNA delivery to the target cells is key. *In vitro* transfection strategies have benefited from the development of formulations to protect mRNA from degradation mediated by RNase and to facilitate cellular uptake [11]. In addition to the cationic lipids [12][13][14][15][16], other investigated chemical delivery systems include cationic polymers, such as polyamidoamine dendrimers and polyethylenimine (PEI).

Among the various types of non-viral vectors, cationic lipids are especially attractive as they can be prepared with relative ease and have been extensively characterized [17][18]. More and more commercial non-viral vectors consisting of cationic lipids are available for *in vitro* mRNA delivery, such as Lipofectamine® 2000 and Lipofectamine® messengerMAX [19][20][21]. In contrast, cationic polymers are hardly investigated for mRNA delivery, although they have been widely exploited with great success for other nucleic acids, such as pDNA, oligonucleotides and siRNA [22]. One of the most widely employed cationic polymers is PEI, due to its advantages such as a strong DNA condensation capacity and buffer capacity, which provides PEI with some endosomal escape ability (proton sponge effect). PEI exists as a linear or branched polymer and can be found with different molecular weights. Among them, linear PEI of 22 kDa and branched PEI of 25 kDa are the most effective transfection reagents used *in vitro* and *in vivo* with pDNA [23][24]. However, high molecular weight PEI also shows relatively considerable toxicity, whereas PEI with low molecular weight has low toxicity but less transfection efficiency. It has been reported that PEI polymers are able to efficiently complex and thus protect unmodified RNA molecules including ribozymes and siRNAs [25]. Only few studies addressed PEI for mRNA delivery, where it was typically less effective [22], potentially due to differences in mRNA-polycation binding compared to pDNA and siRNA [26][27][28][29].

Both cationic polymers and cationic lipids face barriers to gene delivery [30]. The mRNA delivery systems should have high transfection efficiency, low cytotoxicity and no immune response [31]. Also, it should achieve a sufficiently high level of the encoded protein and reach a high number of cells. In most transfection studies, complexes are administered to cells in a reduced serum condition such as Opti-MEM when evaluating their stability, uptake, intracellular trafficking and transfection. It is well-established, however, that once in contact with protein-rich biological fluids, most nanoparticles are spontaneously covered by a layer of biomolecules with the formation of a so-called “protein corona” [32][33][34]. This corona might seriously affect the performance of complexes, both on the level of extracellular stability, cell targeting, cellular uptake and intracellular trafficking [35][36]. Therefore, performing *in vitro* optimization of nano-sized formulations in undiluted biological fluids before assessing the functionality *in vivo* is always advised [37]. Clearly, a good delivery system should maintain a critical balance between complexing the mRNA in the extracellular environment, but releasing it inside the cytoplasm of the cells. The association and dissociation from mRNA to a certain carrier is mostly investigated by gel electrophoresis. This analytical tool, however, is not applicable to explore the stability and integrity of mRNA-carrier complexes in biological fluids, as proteins and nucleic acids in the biological fluid interfere with the read-out of the gels [26][27][28][29][38][39][40].

Our research group has reported before that FCS is a valuable tool to explore the delivery of short antisense oligonucleotides and siRNA (21 nucleotides) with lipid-based and polymer-based carriers:

both the protection of the nucleic acids against enzymatic degradation and the association and dissociation of the nucleic acids from the carriers can be followed in buffer, in biological fluids such as human serum and intraperitoneal fluids and inside living cells [41][42][43]. The applicability of FCS to explore complex characteristics between carriers and much longer nucleic acids such as mRNA (1000 nucleotides), however, has not been reported before. In the present study, we aimed to evaluate whether FCS can be used to explore the stability of mRNA-complexes in buffer and in biological fluids. Lipofectamine[®] messengerMAX and linear PEI were chosen as representative lipid- and polymer-based carriers to complex mRNA into lipoplexes and polyplexes, respectively. We found that FCS is able to measure the degree of association and dissociation of mRNA-based complexes in buffer, full human serum and human ascitic fluid in a few minutes, while gel electrophoresis resulted in reliable measurements only in buffer. Furthermore, we evaluated the transfection efficiency of the mRNA-complexes in low-protein and high-protein conditions and attempted to correlate the results with differences in mRNA binding and release, as determined by FCS. The lipid-based carrier used in this study was more efficient when compared to linear PEI that failed to release the complexed mRNA in the cytoplasm of the cells. Therefore, a critical balance should be maintained between complexing the mRNA in the extracellular environment, without compromising the ability of the carrier to release its cargo into the cytoplasm of the cells.

2. Materials & Methods

2.1 Consumables

Lipofectamine[®] MessengerMAX and linear jetPEI (average Mw 22kDa) were purchased from Invitrogen (Merelbeke, Belgium) and Polyplus-transfection[®] SA (Strasbourg, France), respectively. mRNA encoding GFP labeled by Cyanine 5 (ARCA capped, 25% Cyanine 5-U, 75% Pseudo-U, 100% 5-Me-C) was purchased from Trilink (California, USA). HEPES, sucrose, sodium dodecyl sulfate and dextran sulfate with Mw's of 50 kDa were purchased from Sigma-Aldrich (Belgium). McCoy's 5A modified Medium, Opti-MEM, 0.25% Trypsin-EDTA (1×), penicillin-streptomycin (5000 U/ml) and DPBS [-] (no calcium, no magnesium) were purchased from Invitrogen (Merelbeke, Belgium).

2.2 Collection of biological fluids

Human serum was obtained from healthy volunteers. Blood was collected into Venosafe[™] 6 ml tubes containing gel and clotting activator (Terumo Europe[™], Leuven, Belgium) at Ghent University hospital. Then the tubes were centrifuged for 10 minutes with a speed of 4000× g at 20°C. The supernatant (serum) was aliquoted (50 µl) in sterile polypropylene tubes and stored at -20°C and thawed at 4°C overnight prior to use. Human ascitic fluid was obtained from patients diagnosed with peritoneal carcinomatosis at the department of medical oncology, Ghent University hospital, with approval of the ethics committee of the Ghent University hospital (ECD no. 2013/589).

2.3 Association degree (%) of complexes in HEPES buffer measured by gel electrophoresis and FCS

To study the complexation of mRNA and linear PEI (linPEI) by agarose gel electrophoresis and FCS, 5 µl PEI solution (the concentration of PEI depending on the desired N/P ratio of 0, 0.25, 0.5, 1, 2, 5, 10, 15, 20, 30) was added to 5 µl mRNA (80 µg/ml), vortexed for 15 s and incubated at room temperature for 30 min prior to use. messengerMAX/mRNA complexes were prepared as following: messengerMAX solution (the volume depending on the desired v/w ratio (volume (µl)/weight(µg)), namely 0, 0.25, 0.5, 1, 2, 3, 5, 10) was mixed with HEPES buffer (pH7.4, 20 mM) to a total volume of 5 µl and incubated at room temperature for 10 min prior to use. Then, 5 µl of the messengerMAX solution was added to 5 µl mRNA (80 µg/ml) and mixed well, followed by incubation at room temperature for 30 min. After incubation, 20 µl HEPES buffer (pH7.4, 20 mM) was added to the different complexes to result in 30 µl of complex solution.

For gel electrophoresis, 11.3 µl of this solution was diluted with HEPES buffer (pH7.4, 20 mM) to a total volume of 25 µl and loaded on a 1% agarose gel after addition of 5 µl of 50% sucrose. The gel was run

for 30 min at 100 V before imaging. The association degree of mRNA was calculated by measuring the amount of free mRNA on the gel with Image J. For FCS measurements, the remaining complex solution (18.7 μ l) was diluted with HEPES buffer (pH7.4, 20 mM) to a total volume of 50 μ l.

2.4 Dissociation degree (%) of complexes in HEPES buffer measured by gel electrophoresis and FCS

10 μ l complex solution was prepared as described above (linPEI/mRNA with N/P ratio of 5, and messengerMAX/mRNA with v/w ratio of 3). At the end of incubation, increasing amounts of sodium dodecyl sulfate (SDS) and dextran sulfate (DS) were added to 10 μ l of lipoplexes and polyplexes, respectively. Then the mixture was diluted with HEPES buffer (pH7.4, 20 mM) to a total volume of 30 μ l and incubated at room temperature for 10 min. For gel electrophoresis, 11.3 μ l of this solution was diluted with HEPES buffer (pH7.4, 20 mM) to a total volume of 25 μ l and loaded on the 1% agarose gel after addition of 5 μ l of 50% sucrose. The gel was run for 30 min at 100 V before imaging. For FCS measurements, the remaining complex solution (18.7 μ l) was diluted with HEPES buffer (pH7.4, 20 mM) to a total volume of 50 μ l.

2.5 Complex stability in biological fluids and cell lysate measured by gel electrophoresis and FCS

14 μ l complex solution (i.e. messengerMAX/mRNA with v/w ratio of 1, 3, and 5, linPEI/mRNA with N/P ratio of 1, 5 and 10) was prepared by mixing an equal volume of mRNA (200 μ g/ml) and messengerMAX and linPEI, respectively. For gel electrophoresis, 2.5 μ l of this complex solution was added to 22.5 μ l HEPES buffer (pH7.4, 20 mM), human serum, human ascitic fluid or cell lysate respectively and incubated at 37°C for 1 h. Then, the samples were loaded on 1% agarose gel after the addition of 5 μ l of 50% sucrose. For FCS measurements, 8 μ l of the complex solution was diluted with 8 μ l HEPES buffer. 5 μ l of this diluted complex solution was mixed with 45 μ l HEPES buffer (pH7.4, 20 mM), human serum, human ascitic fluid or cell lysate, respectively, and incubated for 1 h at 37°C prior to measurement. Cell lysate was prepared by resuspending a cell pellet of SKOV-3 cells (150000 cells/well) in 1 ml RIPA buffer (Sigma-Aldrich, Belgium). After 30 minutes incubation on ice, cells were crushed by pipetting up and down using 21G needles. The cell lysate was kept at -80°C until use.

2.6 Charge and size characterization of mRNA complexes

The average size and ζ potential of lipoplexes with varying v/w ratios and polyplexes with varying N/P ratios was measured using Zetasizer Nano-ZS (Malvern, Worcestershire, UK) in HEPES buffer. Complexes were allowed to form during 30 minutes at room temperature, after which they were diluted with 20 mM HEPES buffer (pH7.4) to a final concentration of 0.3 μ g/ml mRNA. All measurements are shown in Supplementary Figure 1. Both lipoplexes and polyplexes varied between 300 and 600 nm and were negatively charged for all tested ratios.

2.7 Cell culture

The human ovarian cancer cell line SKOV-3 was used for *in vitro* experiments. SKOV-3 cells were cultured in McCoy's 5A medium supplemented with 10% Fetal Bovine Serum (FBS) and penicillin-streptomycin. Cells with 80%-90% confluency were detached from the bottom of the cell culture flask with 0.25% trypsin/EDTA. Cells were maintained in an incubator at 37°C in a humidified atmosphere containing 5% CO₂.

2.8 Cellular uptake and transfection

SKOV-3 cells (50 000 cells/well) were cultured in 24-well plates at 37°C, 5% CO₂ for 24 h before treatment. Before incubation with complexes, cells were washed with DPBS [-] (500 μ l/well) and cultured with 440 μ l Opti-MEM for each well except for the control group which contained 500 μ l culture medium. Complexes were added to Opti-MEM, human serum or human ascitic fluid to a final concentration of 80% biological fluids and pre-incubated at 37°C for 1 h. At the end of pre-incubation, 60 μ l mixture containing 0.3 μ g mRNA was incubated with SKOV-3 cells in each well for 4 h for uptake and 24 h for transfection at 37°C, 5% CO₂, respectively. After 4 h or 24 h incubation, cells were rinsed

with DPBS [-] (500µl/well), trypsinized (trypsin/EDTA 0.25%) and diluted with culture medium. Following centrifugation (5 min, 500 g), the cell pellet was resuspended in 300 µl flow buffer (PBS supplemented with 1% BSA and 0.1% sodium azide) and placed on ice until flow cytometry analysis. A minimum of 5 000 cells were analyzed in each measurement by using a flow cytometry (FACSCalibur, BD Biosciences Benelux N.V., Erembodegem, Belgium).

2.9 Cell viability assay

The MTT assay was used to examine the cell viability following incubation of the studied formulations as well as the carriers. SKOV-3 cells (50 000 cells/well) were cultured in 24-well plates at 37°C in a humidified atmosphere containing 5% CO₂ for 24 h before treatment. Cells incubated with culture medium and 70% ethanol (in culture medium) were used as negative (alive) and positive (dead) control, respectively. Other cells were incubated with 60 µl complexes or solution only containing carriers at 37°C, 5% CO₂ for 4 h. Afterwards, the cells were washed with DPBS [-] (500 µl/well), and fresh culture medium was added for overnight incubation. After 24 h incubation, 500 µl MTT (1 mg/ml) was added to the cells in every well and incubated at 37°C, 5% CO₂ for 3 h. At the end of incubation, the MTT solution was aspirated and 500 µl DMSO was added to each well to dissolve the formazan crystals. The plates were covered with aluminum foil and placed on an orbital shaker for 30 min with 100 rpm. The absorbance of the formed formazan crystals at 560 nm and 650 nm was measured using a Wallac Envision™ multilabel reader (PerkinElmer, Zaventem, Belgium). Cell viability (%) for each sample was calculated as follows:

$$\text{cell viability (\%)} = \frac{(A_E - A_C)}{(A_N - A_C)} \times 100\%$$

where A_E , A_N and A_C are the absorbance of experimental groups, negative groups and positive groups (i.e. control groups) respectively.

2.10 Image J analysis

To analyze the images obtained from gel electrophoresis by Image J, identical rectangular areas were selected for each well at the level of intact mRNA (determined with the free mRNA control). The fluorescence intensity of each rectangular area was quantified by the software, corresponding to the amount of free mRNA. Then the association or dissociation degree (%) was calculated in relation to the control free mRNA.

2.11 Fluorescence Correlation Spectroscopy (FCS)

The association and dissociation of fluorescently labeled mRNA to non-labeled carriers in buffer and biological fluids was studied by single-color FCS. FCS is a fluorescence microscopy based technique to measure the continuous movement of fluorescent single molecules in and out of the detection volume, which induces fluorescence fluctuations [43][44][45][46][47]. Fluorescence time traces were obtained by focusing a 640 nm laser line through a water immersion objective lens (60x Plan Apo VC, N.A. 1.2, Nikon, Japan) at about 50 µm above the bottom of the glass-bottom 96-well plate (Grainer Bio-one, Frickenhausen, Germany), which contained the samples (50 µl). The use of a confocal microscope (Nikon C1) ensured only the fluorescent light coming from a small volume (by calibration with a rhodamine green fluorophore, about 1.9 µm in height and a half width of 0.2 µm) was collected. The fluorescence signal was recorded by a photon counting instrument (PicoHarp 300, PicoQuant). A time trace was obtained by binning the photon counts in intervals of 60 s. The fluorescence baseline of the time trace was calculated from the empirical fluorescence distribution as the fluorescence value at which the distribution is rejected by the Lilliefors test for normality (95% confidence interval). The fluorescence baseline of each mixture (Figure 1A, naked mRNA; Figure 1B, mRNA complex) was corrected for any background by subtracting the background fluorescence of a blank sample (Figure 1C, background-C) and a relative baseline is obtained by dividing the fluorescence baseline by the

fluorescence baseline of free mRNA at the same concentration. This relative baseline is directly proportional to the fraction of free mRNA and serves as a measure for the association/dissociation degree of the complexes, as Figure 1 shows.

2.12 Statistical analysis

Results are shown as mean \pm standard deviation. Experiments were performed at least in triplicate on independent days. Significance between the means of two groups was tested using 2-way ANOVA with the software GraphPad Prism 7. A P-value < 0.05 was considered to be significant.

3. Results and discussion

3.1 FCS can determine the association degree (%) of mRNA-complexes in HEPES buffer

Figure 2 shows the association of mRNA with the lipid-based carrier messengerMAX, as followed by gel electrophoresis and FCS. From the gel (Figure 2A), it is clear that full complexation of the mRNA starts from v/w ratio 3, as naked mRNA is no longer detected on the gel. Using FCS, full complexation is confirmed (Figure 2C). Indeed, while naked mRNA results in fluorescence fluctuations around an average of 200 kHz (Figure 2B, red line), highly intense fluorescence peaks appear in the fluctuation profiles of the complexes at v/w ratio 3 (Figure 2B, blue line), corresponding to highly fluorescent complexes which contain multiple mRNA molecules per complex. Also, the fluorescence baseline dropped from 207 ± 27 kHz ($\sim 100\%$ naked mRNA) to 16 ± 5 kHz ($\sim 7\%$ of naked mRNA), upon complexation. As the baseline fluorescence correlates with the fraction of remaining naked mRNA, this drop again shows the binding of the mRNA to the messengerMAX. Analyzing the association degree based on this drop of the fluorescence baseline shows that FCS is equally accurate when compared to gel electrophoresis to determine the amount of associated mRNA (Figure 2C). Furthermore, the height and the broadness of the peaks in the FCS profiles give extra insight on the complex characteristics. Figure 2D, for example, demonstrates that upon increasing the v/w ratio from 3 to 10, the fluorescence baseline remains low, but fluorescence peaks become less intense. This suggests that a lower amount of mRNA molecules is present per complex, in agreement with the expectation that the mRNA molecules can distribute over more messengerMAX/mRNA complexes when a higher v/w ratio is used.

Apart from the lipid-based carrier messengerMAX, also the widely used polymeric carrier linear PEI was followed by gel electrophoresis and FCS. For linPEI, diffusion of naked mRNA into the agarose gel is no longer observed from lane 5 (N/P ratio 3), as indicated by the arrow in Figure 3A. When these samples were analyzed with FCS, again the fluorescence baseline dropped in comparison with naked mRNA (Figure 3B, red line), demonstrating mRNA was complexed. Remarkably, however, highly intense fluorescence peaks do not appear in the fluctuation profiles (Figure 3B, blue line). This indicates that linPEI strongly condenses the mRNA molecules, thereby quenching their fluorescence and making the complexes invisible for the FCS detectors. From the drop of fluorescence baseline, however, the association degree of mRNA to linPEI can be calculated in function of the N/P ratio. Also from the gels, the amount of complexed mRNA was calculated with Image J. Figure 3C shows that for linPEI up until N/P ratio 15, both gel electrophoresis and FCS show the same trend for the calculated association degree. A decrease in complexation efficiency seems to occur, however, with higher N/P ratios when calculated by FCS, while the agarose gel still shows full complexation. An explanation for this phenomenon can be found by analyzing the fluorescence fluctuation profiles of linPEI at higher N/P ratios (Figure 3D). First, the fluorescence baseline gradually increases with increasing N/P ratios. Second, fluorescence peaks appear in the fluctuation profiles only at higher N/P ratios. These observations suggest that mRNA fluorescence is quenched in the complexes at lower N/P ratios, but gradually recovers by increasing the N/P ratio. Therefore, this dequenching and corresponding increase in baseline fluorescence represents the mRNA distribution over more PEI complexes and not an actual decomplexation of mRNA at higher N/P ratios.

3.2 mRNA dissociation from lipid- and polymer-based complexes

The dissociation of mRNA from complexes is essential to obtain free mRNA that is translated into proteins in the cytoplasm of the cells [48]. The mRNA dissociation from the lipid based messengerMAX/mRNA complexes was investigated by gel electrophoresis and FCS after the addition of the surfactant sodium dodecyl sulfate (SDS), which induces the release of mRNA by dissolving the lipoplexes. Gel electrophoresis clearly demonstrates the gradual release of mRNA with increasing amounts of SDS, reaching full dissociation with 10 μg SDS per 0.4 μg messengerMAX/mRNA complexes (Figure 4A). Also FCS was able to follow the dissociation of mRNA in function of the SDS amount by a gradual increase in the baseline of the fluorescence fluctuations upon the release of mRNA from the complexes, accompanied with a decrease in the amount of fluorescence peaks in the fluorescence fluctuations profiles (Figure 4B, D).

To dissociate the mRNA from the PEI-based complexes, negatively charged dextran sulfate (DS) was added to the polyplex dispersions to compete with mRNA for binding to the PEI. As Figure 5A demonstrated, (partial) dissociation of mRNA from the complexes was indeed observed by agarose gel electrophoresis. Release of mRNA from linPEI started from sample 2 containing 5 μg DS, with about 60% of mRNA released (Figure 5C). The maximal percentage of released mRNA (around 80%) was reached at 10 μg DS (lane 4), followed by a gradual decrease until 200 μg of DS.

3.3 Stability of mRNA-complexes in undiluted biological fluids and cell lysate

Biological fluids, such as human serum and human ascitic fluid, contain several negatively charged molecules (e.g. albumin) that might compete with mRNA binding to positively charged carriers. Therefore, the ability of complexes to retain the complexed mRNA in the presence of human serum and human ascitic fluid was evaluated by agarose gel electrophoresis and FCS (Figure 6). As a comparison, the amount of complexed mRNA in HEPES buffer is also depicted. Gel electrophoresis clearly shows that the biofluids themselves give a background signal on the agarose gel, resulting in a huge smear on the gel, probably due the presence of proteins, DNA or RNA in the serum and human ascitic fluid (Figure 6A, B, lane 10 and 15)[45]. Also, naked mRNA can no longer be detected on the gel in the presence of biofluids. As a consequence, gel electrophoresis is no longer suited to quantify the mRNA complexation efficiency in the presence of serum and human ascitic fluid.

When analyzing the same samples by FCS, the shortcomings of gel electrophoresis could be overcome as FCS was able to quantify the amount of free mRNA in mRNA-carrier dispersions, even in the presence of biological fluids. This results from the fact that FCS only detects the fluorescent mRNA, so that the presence of proteins and other macromolecules does not interfere with the readout of the fluorescence fluctuations. It should be noted that naked mRNA is degraded in the presence of biofluids, resulting in an increase of the fluorescence intensity of free mRNA (Supplementary Figure 2). As also the mRNA released from complexes is degraded, however, this does not interfere with the calculation of complex efficiency based on FCS measurements. Figure 6C and 6D demonstrate that the incubation of mRNA complexes in biological fluids induces a partial dissociation of the mRNA from the complexes. In general, human ascitic fluid displaced more mRNA molecules from the complexes than human serum, especially for complexes with a suboptimal carrier/mRNA ratio, while increasing the carrier/mRNA ratio makes the complexes more resistant against both human serum and human ascitic fluid. Also, the linPEI/mRNA complexes release more mRNA in ascitic fluid when compared to messengerMAX/mRNA, especially for the highest ratios (N/P ratio 10 and v/w ratio 5, respectively). To estimate the ability of complexes to release mRNA in the intracellular environment, we have performed stability measurements of complexes in cell lysate. LinPEI/mRNA with N/P 5 and 10 only released about 5% of mRNA after incubation in cell lysate at 37°C for 1 hr, while around 50% and 30% of mRNA released from lipoplexes with v/w 3 and 5, respectively. Therefore, it seems that linPEI/mRNA complexes are less stable in the extracellular biofluids, but more stable in the intracellular environment.

3.4 Intracellular mRNA delivery is less productive for PEI based complexes when compared to messengerMAX

To evaluate the cellular entry and transfection properties of complexes, Cy5 (red fluorescence) labeled mRNA encoding for enhanced green fluorescence protein (GFP, green fluorescence) was used. The uptake of complexes was followed after 4 hours of incubation with the cells, while the expressed GFP signal was studied after 24 h. All complexes used did not exhibit any severe decrease in the cell viability (Supplementary Figure 3).

Figure 7 shows the uptake and transfection efficiency obtained for messengerMAX/mRNA and linPEI/mRNA complexes in Opti-MEM. Cellular entry is the first important step in the transfection pathway. Figure 7 shows uptake in almost 100% of the cells, irrespective of the carrier/mRNA ratio or the type of carrier that was used (Figure 7A, D, Cy5). The mean fluorescence intensity (MFI) of Cy5 per cell, however, did vary with the type of carrier. Complexes of messengerMAX/mRNA with v/w ratio 3 and 5 resulted in a MFI around 7000 (Figure 7B, Cy5), while for linPEI/mRNA prepared at N/P ratio 5 and 10, the amount of mRNA delivered to each cell seems lower, with a MFI around 3500 (Figure 7E, Cy5). It should be noted, however that this MFI might be an underestimation due to the quenching of Cy5 fluorescence in linPEI/mRNA complexes. MFI of Cy5 in the cells transfected with messengerMAX/mRNA (v/w ratio 1) and linPEI/mRNA (N/P ratio 1) at suboptimal ratios was around 3000 and 1000, respectively, which is much lower than that of analogues with higher carrier/mRNA ratios ($P=0.0063$, **; $P<0.0001$, ****). As flow cytometry only measures the overall Cy5 fluorescence, irrespective of the cellular compartment in which the Cy5-labeled mRNA is present, we additionally performed FCS measurements in the cytoplasm of the cells transfected by carriers with an intermediate ratio. As Supplementary Figure 4 demonstrates, messengerMAX/mRNA complexes deliver on average 10 times more mRNA to the cytoplasm when compared to linPEI/mRNA complexes at the 4 hour time point. Also, GFP expression can already be detected in all cells treated with messengerMAX/mRNA complexes, while it remains at background level for cells treated with linPEI/mRNA complexes. This indicates mRNA is more efficiently delivered to the cytoplasm of the cells when messengerMAX/mRNA complexes are used.

The ability of the internalized mRNA to induce GFP expression was additionally determined after 24 h by flow cytometry. Around 93% of the cells transfected with messengerMAX showed expression of the GFP, demonstrating the delivery of free mRNA into the cytoplasm of the cells (Figure 7A, GFP). The MFI, however, clearly demonstrates that the intermediate carrier/mRNA ratio 3 results in the higher amount of GFP expression per cell (Figure 7B, GFP, gray bars), indicating that the release of mRNA in the cytoplasm of the cell was more optimal for this carrier/mRNA ratio. For linPEI/mRNA complexes, GFP expression was seen in about 65% of the cells treated with N/P ratio 5 and 10 (Figure 7D, GFP), which was significantly higher than that of polyplexes with N/P 1 ($P<0.0001$, ***). Again, the MFI of GFP was slightly higher for complexes with the intermediate N/P ratio 5, when compared to those with a N/P ratio 1 and 10, although the MFI per cell was clearly much lower when compared to messengerMAX. The difference between the lipids- and polymer-based mRNA delivery is also clearly visible from Figure 7C, F. Indeed, the GFP fluorescence intensity of cells transfected with messengerMAX/mRNA complexes clearly outperforms those from linPEI/mRNA complexes, even though the cellular entry of Cy5 labeled mRNA is visible as intracellular red fluorescent dots. Taken together, these data demonstrate that the amount of mRNA delivered per cell is comparable for the lipid-based messengerMAX and polymer-based linPEI-complexes, but is much more efficiently transcribed into GFP when messengerMAX is used, both at the 4 h and 24 h time point.

3.5 Biofluids decrease uptake and transfection efficiency of PEI based complexes but not of messengerMAX

Considering the fact that *in vivo*, the complexes for *IV* or *IP* administration can come into contact with human serum and human ascitic fluid, we also evaluated whether a 1 h pre-incubation of the complexes in the biological fluids would influence their uptake and transfection efficiency (Figure 8).

The pre-incubation with biofluids does not significantly lower the uptake or transfection efficiency of the messengerMAX complexes with v/w 3 and 5, when compared to Figure 7A, B. Again about 100% of the cells internalize mRNA (Figure 8A, C, Cy5), with a MFI comparable to the one obtained in Opti-MEM (Figure 8B, D, Cy5). More than 90% of the complexes express GFP in the presence of the biofluids (Figure 8A, C, GFP), and the v/w ratio 3 is most effectively translated into the GFP protein (Figure, 8B, D, GFP, grey bars). For linPEI/mRNA complexes, the presence of human serum and human ascitic fluid, does not influence the number of Cy5 positive cells when compared to Opti-MEM (Figure 8E, G, Cy5), but clearly lowers the amount of mRNA delivered per cell (Figure 8F, H, Cy5). When looking at the GFP expression, however, the drastic effect of both human serum and ascitic fluid becomes evident as both the percentage of transfected cells (Figure 8E, G, GFP) and the MFI per cell (Figure 8F, H, GFP) decreased to background levels (<1%) in the presence of the biofluids. These results correspond to the lower stability of linPEI/mRNA complexes in biofluids when compared to messengerMAX/mRNA complexes, as observed in Figure 6.

4. Discussion

Nucleic acids (including DNA, oligonucleotides, siRNA, shRNA, mRNA...) have been loaded on vectors as therapeutics for various diseases. Vectors, like cationic lipids and cationic polymers, can not only transport nucleic acids to the target cells, but also protect nucleic acids from degradation mediated by enzymes present in the extracellular and intracellular environment. To obtain an efficient delivery system of nucleic acids-based therapeutics, a critical balance between complexing the nucleic acids in the extracellular environment and releasing functional nucleic acids into the cytoplasm or nucleus of the target cells is required. The most typical method to evaluate the stability of complexes, is gel electrophoresis. This method, however, does not allow to study the stability of complexes in biological fluids since the background signal and nuclease activity interferes with the readout of the gel. Previously, we showed that FCS is a good method to follow stability of siRNA and oligonucleotide containing complexes in buffer, biofluids and living cells [41][49]. In this paper, we demonstrated that FCS is also applicable to follow the association and dissociation of larger nucleic acids such as mRNA to lipid- and polymer-based carriers. The read-out can be performed within minutes without the need to separate non-encapsulated mRNA from the complexed fraction. Also, as FCS only detects the fluorescently labeled mRNA of interest, there is no interference from mRNA or other nucleic acids present in biofluids.

In this study, mRNA was loaded on a positively charged lipid vector (i.e. messengerMAX) or complexed with positively charged polymers (i.e. linPEI). Lipoplexes of messengerMAX/mRNA showed full complexation starting from v/w ratio 3 (Figure 2). The presence of complexes was evident from the appearance of fluorescence peaks in the fluctuations profiles, as several fluorescently labeled mRNA molecules are present in a single complex. This is in agreement with our previous observations when complexing fluorescently labeled oligonucleotides or siRNA to DOTAP/DOPE liposomes [41][50]. Also in agreement with previous observations, SDS was able to dissociate the mRNA from the complexes. When the messengerMAX/mRNA complexes were incubated in biofluids, more than 50% of the encapsulated mRNA was released in case of v/w ratio 1 and 3, while this was only 10% for v/w ratio 5. Clearly, increasing the v/w ratio of messengerMAX/mRNA thus increased the resistance against biofluids. This suggests that at higher complexation ratios, mRNA is mainly encapsulated in the lipoplexes' core, while for low or intermediate ratios, half of the complexed mRNA is loosely attached to the surface of the lipoplexes, accessible to competing nucleic acids and macromolecules in the biofluids. Transfection experiments demonstrated that the complexes of v/w ratio 3 showed the higher GFP expression level per cell when compared to v/w ratio 1 ($P=0.0021$, **) and 5 ($P=0.0019$, **). It is well accepted that cationic lipoplexes enter cells by endocytosis, followed by endosomal escape. Typically, the endosomal escape mechanism that is proposed for lipoplexes is a fusion of the phospholipid bilayer of a liposome with the endosomal membrane. Anionic lipids from the inner face of the endosomal membrane can interact with the cationic lipids from the lipoplexes to form neutralized ion-pairs, allowing cargo release in the cytoplasm during endosomal escape [51]. For

messengerMAX/mRNA complexes, with almost 100% of cellular uptake, a comparable amount of mRNA complexes was transported into cells for v/w ratio 3 and 5 (Figure 7B). For v/w ratio 5, however, the amount of free mRNA that reaches the cytoplasm is apparently less when compared to the analogues with v/w ratio 3 as can be seen by the lower amount of GFP expression in Figure 7B although no significant differences were observed on the level of cellular entry. Possibly, v/w ratio 5 more strongly complexes the mRNA, preventing the efficient release of mRNA during endosomal escape. El Ouahabi et al., for example, demonstrated that the complexation of luciferase encoding mRNA by cationic lipids strongly reduced its accessibility to the translation machinery, with almost a complete loss of luciferase expression at w/w ratios over 4 in a cell-free translation system [52], indicating that only free mRNA is efficiently transcribed to GFP. Alternatively, a lower amount of expressed protein could result from a different stimulation of immune responses by the encapsulated mRNA or the amount of lipids present in the complexes. mRNA is known to be able to stimulate the endosomal toll-like receptor 3 and 7/8 [2]. However, as the mRNA in complexes with v/w ratio 5 is expected to be less exposed on the outside of the lipoplexes, it seems less likely that complexes with v/w ratio 5 are more immune stimulatory than those with v/w ratio 3. Therefore, we assume that mainly the dissociation of mRNA is the factor that determines the better transfection efficiency of lipoplexes with v/w ratio 3. Interestingly, the cellular internalization of complexes and the resulting transfection efficiency did not lower significantly after the pre-incubation of lipoplexes with biological fluids such as human serum ($P=0.6987$) and ascitic fluid ($P=0.989$) (Figure 8 A-D, compared to Figure 7A-D). Therefore, messengerMAX/mRNA complexes with v/w ratio 3 seem good candidates for *in vivo* delivery of mRNA as well.

Apart from lipid-based carriers, polyplexes of linPEI/mRNA were prepared with increasing N/P ratios. From gel electrophoresis, full complexation was observed from N/P ratio of 3 (Figure 3). However, from FCS measurements, an “apparent decrease in complexation efficiency” was found for linPEI/mRNA at higher N/P ratios. An explanation for this apparent decomplexation can be found when looking at the fluorescence fluctuation profiles. In contrast to lipid-based complexes, no fluorescent peaks appeared in the fluorescence fluctuation profiles when using linear PEI polymers at N/P ratio 3. As gel electrophoresis demonstrated that all mRNA was bound into polyplexes at these N/P ratios, the absence of fluorescence peaks indicates that the complexed Cy5 labeled mRNA is quenched, rendering the complexes invisible for the FCS instrument. This quenching typically occurs when the fluorescent labels on the complexed nucleic acids are tightly packed together in the polyplexes’ core, and was observed before for oligonucleotides as well [50]. With higher N/P ratios, the fluorescence fluctuation profiles changed as fluorescence peaks occurred and a gradual increase in the fluorescence baseline was observed. Both phenomena point to a gradual dequenching as the fluorescently labeled mRNA distributes differently over PEI complexes at a higher N/P ratio. For PEI complexes containing more than one fluorescently labeled mRNA molecule, dequenching results in the appearance of fluorescence peaks. Dequenching, however also results in the increase of the fluorescence baseline as more mono-molecular complexes are formed, containing a single fluorescently labeled mRNA per complex. As the PEI polymers themselves are not fluorescently labeled, these mono-molecular complexes are misinterpreted as released free mRNA.

When PEI complexes were incubated with biofluids, gel electrophoresis was no longer suitable to measure the association or dissociation degree (Figure 6B). Using FCS, however, it was observed that linPEI/mRNA complexes with an intermediate N/P ratio of 5 release up to 50% and 80% of the complexed mRNA in the presence of human serum and human ascitic fluid respectively (Figure 6D). Increasing the N/P ratio make polyplexes more stable in the presence of biofluids (Figure 6D). Nevertheless, we observed that cellular uptake of both linPEI/mRNA polyplexes with N/P 5 and 10 was significantly reduced in the presence of human serum (N/P 5, $P=0.032$, *; N/P 10, $P=0.0368$) and human ascitic fluid (N/P 5, $P=0.0186$, *; N/P 10, $P=0.0022$) (Figure 8G, H, Cy5). This decrease in cellular uptake most likely results from the presence of proteins in the biofluids that induce the premature release of

mRNA in the extracellular environment and might additionally form a protein corona around the polyplexes, preventing their cellular uptake.

When compared to mRNA lipoplexes, we observed that less mRNA polyplexes were delivered per cell (Figure 7), which is in agreement with previous studies [19]. We also observed, however, that only a very limited amount of GFP expression was detected per cell in the presence of biofluids (Figure 8F, H, GFP). This phenomena was surprising based on previous research that DNA-containing polyplexes had higher or comparable gene expression than lipid transfection agents and did not reveal serum dependence [53]. PEI with varying molecular weights and forms have been extensively investigated for transfection efficiency and cytotoxicity. It has been reported that the release of nucleic acids such as mRNA may be impaired in these PEI-based complexes [25][54][55]. Also we observed that the MFI of GFP expression was much less when compared to messengerMAX/mRNA complexes, with a MFI of maximum 200 for linPEI/mRNA with N/P ratio 5 when compared to about 5500 for messengerMAX/mRNA complexes with v/w ratio 3 (Figure 7B, E, GFP). It is known that after cellular uptake through endocytosis, PEI polyplexes escape the endosomes by the “proton sponge” effect. The buffering effect of PEI evokes the continuous proton influx in the endosomes, which induces osmotic swelling and rupture resulting in release of the complexed cargo and/or intact polyplexes into the cytoplasm of the cells [25][56]. Once released into the cytosol, polyplexes should dissociate before nucleic acids like mRNA can be translated into the encoded proteins. Based on our observations, this endosomal escape and/or dissociation of the mRNA into the cytosol does not occur for linPEI complexes as no mRNA is detected in the cytoplasm of the cells (Supplementary Figure 4). Furthermore, linPEI/mRNA complexes did not dissociate in the presence of cell lysate (Figure 6). Also others have observed that the dissociation of polyplexes in the cytoplasm seems relatively slow [57]. For example, the intracellular polyplexes of double-labeled PEI/DNA were not dissociated yet after 4 h incubation with B16F10 cells [58], while dissociation of these polyplexes was found after incubated with pancreatic carcinoma cells for 18 h [59]. The mechanisms of polyplexes’ dissociation is still poorly understood even though dissociation of free nucleic acids in the cytoplasm of the cells is required for efficient transfection. Rejman J et al. [19] investigated the endosomal release of linear PEI (22 kDa)/mRNA encoding GFP by using photochemical internalization (PCI) to trigger an oxidative process that leads to disruption of the endosomal membrane and release of material localized in this compartment. The PCI-induced release of polyplexes from the endosomal compartment did not enhance transfection mediated by these complexes, suggesting that especially the dissociation of the mRNA from the polymer may impede its potential in gene delivery. Furtherly, Bettinger T et al. [13] observed that the amount of GFP-positive cells (%) for PEI 25 kDa/mRNA complexes was 0%, compared to 82% for PEI 25 kDa/mRNA in the presence of pAsp, indicating that the induced dissociation of mRNA from the complexes by pAsp made more mRNA available for translation. To address the problem of too strong mRNA binding by PEI, several strategies have been envisaged to favor dissociation of polyplexes in the cytoplasm without compromising the extracellular stability. For example, reducible PLL polymers, which can be degraded in the cells and then facilitate DNA release, were developed and permitted up to 187-fold increase in gene expression [60]. Also, reducible BPEI1.2k-SS complexes were developed to efficiently deliver the siRNA by enhancing the dissociation free siRNA in the cytoplasm without compromising of complexes’ stability [61]. The FCS method proposed in this study is ideally suited to determine the optimal complexation efficiency and stability in the extracellular environment that still allows for good internalization, endosomal escape and release of mRNA into the cytoplasm of the cells. Considering the recently reported poor correlation between the *in vitro* and *in vivo* delivery of nucleic acids, screening the stability of complexes in extracellular fluids is becoming increasingly important [62]. Furthermore, as demonstrated before for small oligonucleotides, the FCS can also be applied in dual-color mode, where both the nucleic acids and the carrier are labeled with two distinct fluorophores [47][63]. Also for mRNA, dual-color FCS is expected to allow us to furtherly investigate the intracellular dissociation of mRNA from its carrier.

5. Conclusion

In this study, we tested the stability of different mRNA-based formulations in HEPES buffer, human serum and human ascitic fluid, as well as the uptake, transfection and cytotoxicity in SKOV-3 cells. We found that FCS is feasible to follow the association/dissociation degree (%) of mRNA complexes both in buffer and biological fluids in a few minutes, which is a major advantage over typical gel electrophoresis. Gel electrophoresis is not only more time-consuming, making it not suitable for monitoring the time-dependent dissociation of mRNA-carrier complexes on the short time scale (e.g. within minutes), it also does not allow to detect intact dissociated mRNA in the presence of biological fluids such as full human serum and human ascitic fluid. We found that mRNA is more strongly bound to PEI-based complexes, leading to quenching of mRNA fluorescence and difficulty to dissociate the mRNA from the complexes in the intracellular environment. This led to very low transfection efficiencies in SKOV-3 cells as the complexed mRNA is not translated into GFP proteins. For lipid-based complexes, the dissociation of mRNA from the carriers with an intermediate complexation ratio resulted in efficient release of mRNA into the cytoplasm of the cells. Furthermore, lipoplexes used in this study were not sensitive to pre-incubation in biological fluids, while the already low efficiency of PEI-based complexes dropped even further in the presence of biofluids. Taken together, our data demonstrate that it is useful to screen complex stability in extracellular fluids and that we should maintain a critical balance between extracellular stability (in undiluted biofluids) and intracellular cargo release for optimization of nanoparticles formulations.

Acknowledgements

Heyang Zhang gratefully acknowledges the financial support from the China Scholarship Council (CSC) and Dr. Brans for the FCS tutorial and sharing his expertise on the FCS analysis.

Disclosures

No conflicts of interest.

Reference:

- [1] M.S.D. Kormann, G. Hasenpusch, M.K. Aneja, G. Nica, A.W. Flemmer, S. Herber-jonat, M. Huppmann, L.E. Mays, M. Illenyi, A. Schams, M. Griese, I. Bittmann, R. Handgretinger, D. Hartl, J. Rosenecker, C. Rudolph, Expression of therapeutic proteins after delivery of chemically modified mRNA in mice., *Nat. Biotechnol.* 29 (2011) 154–157. doi:10.1038/nbt.1733.
- [2] J. Devoldere, H. Dewitte, S.C. De Smedt, K. Remaut, Evading innate immunity in nonviral mRNA delivery: Don't shoot the messenger, *Drug Discov. Today.* 21 (2016) 11–25. doi:10.1016/j.drudis.2015.07.009.
- [3] K.K.L. Phua, K.W. Leong, S.K. Nair, Transfection efficiency and transgene expression kinetics of mRNA delivered in naked and nanoparticle format, *J. Control. Release.* 166 (2013) 227–233. doi:10.1016/j.jconrel.2012.12.029.
- [4] N. Pardi, S. Tuyishime, H. Muramatsu, K. Kariko, B.L. Mui, Y.K. Tam, T.D. Madden, M.J. Hope, D. Weissman, Expression kinetics of nucleoside-modified mRNA delivered in lipid nanoparticles to mice by various routes, *J. Control. Release.* 217 (2015) 345–351. doi:10.1016/j.jconrel.2015.08.007.
- [5] G. Tavernier, O. Andries, J. Demeester, N.N. Sanders, S.C. De Smedt, J. Rejman, mRNA as gene therapeutic: How to control protein expression, *J. Control. Release.* 150 (2011) 238–247. doi:10.1016/j.jconrel.2010.10.020.
- [6] P. Qiu, P. Ziegelhoffer, J. Sun, N.S. Yang, Gene gun delivery of mRNA in situ results in efficient transgene expression and genetic immunization., *Gene Ther.* 3 (1996) 262–268.

- [7] O. Levy, W. Zhao, L.J. Mortensen, S. Leblanc, K. Tsang, M. Fu, J.A. Phillips, V. Sagar, P. Anandakumaran, J. Ngai, C.H. Cui, P. Eimon, M. Angel, C.P. Lin, M.F. Yanik, J.M. Karp, e- Blood mRNA-engineered mesenchymal stem cells for targeted delivery of interleukin-10 to sites of inflammation, *Blood*. 122 (2013) 23–32. doi:10.1182/blood-2013-04-495119.O.L.
- [8] R.J. Creusot, P. Chang, D.G. Healey, I.Y. Tcherepanova, C.A. Nicolette, C.G. Fathman, A short pulse of IL-4 delivered by DCs electroporated with modified mRNA can both prevent and treat autoimmune diabetes in NOD mice., *Mol. Ther.* 18 (2010) 2112–20. doi:10.1038/mt.2010.146.
- [9] L. Zangi, K.O. Lui, A. von Gise, Q. Ma, W. Ebina, L.M. Ptaszek, D. Später, H. Xu, M. Tabebordbar, R. Gorbatov, B. Sena, M. Nahrendorf, D.M. Briscoe, R.A. Li, A.J. Wagers, D.J. Rossi, W.T. Pu, K.R. Chien, Modified mRNA directs the fate of heart progenitor cells and induces vascular regeneration after myocardial infarction., *Nat. Biotechnol.* 31 (2013) 898–907. doi:10.1038/nbt.2682.
- [10] Y. Wang, H.-H. Su, Y. Yang, Y. Hu, L. Zhang, P. Blancafort, L. Huang, Systemic delivery of modified mRNA encoding herpes simplex virus 1 thymidine kinase for targeted cancer gene therapy., *Mol. Ther.* 21 (2013) 358–67. doi:10.1038/mt.2012.250.
- [11] U. Sahin, K. Karikó, Ö. Türeci, mRNA-based therapeutics — developing a new class of drugs, *Nat. Rev. Drug Discov.* 13 (2014) 759–780. doi:10.1038/nrd4278.
- [12] R.W. Malone, P.L. Felgner, I.M. Verma, Cationic liposome-mediated RNA transfection., *Proc. Natl. Acad. Sci. U. S. A.* 86 (1989) 6077–81. doi:10.1073/pnas.86.16.6077.
- [13] T. Bettinger, R.C. Carlisle, M.L. Read, M. Ogris, L.W. Seymour, Peptide-mediated RNA delivery: a novel approach for enhanced transfection of primary and post-mitotic cells., *Nucleic Acids Res.* 29 (2001) 3882–91. doi:10.1093/nar/29.18.3882.
- [14] F.T. Zohra, E.H. Chowdhury, S. Tada, T. Hoshiba, T. Akaike, Effective delivery with enhanced translational activity synergistically accelerates mRNA-based transfection, *Biochem. Biophys. Res. Commun.* 358 (2007) 373–378. doi:10.1016/j.bbrc.2007.04.059.
- [15] J.F. Nabhan, K.M. Wood, V.P. Rao, J. Morin, S. Bhamidipaty, T.P. LaBranche, R.L. Gooch, F. Bozal, C.E. Bulawa, B.C. Guild, Intrathecal delivery of frataxin mRNA encapsulated in lipid nanoparticles to dorsal root ganglia as a potential therapeutic for Friedreich’s ataxia., *Sci. Rep.* 6 (2016) 20019. doi:10.1038/srep20019.
- [16] D.M. Anderson, L.L. Hall, A.R. Ayyalapu, V.R. Irion, M.H. Nantz, J.G. Hecker, Stability of mRNA/cationic lipid lipoplexes in human and rat cerebrospinal fluid: methods and evidence for nonviral mRNA gene delivery to the central nervous system., *Hum. Gene Ther.* 14 (2003) 191–202. doi:10.1089/10430340360535751.
- [17] M.S. Al-Dosari, X. Gao, Nonviral gene delivery: principle, limitations, and recent progress., *AAPS J.* 11 (2009) 671–681. doi:10.1208/s12248-009-9143-y.
- [18] B. Martin, M. Sainlos, A. Aissaoui, N. Oudrhiri, M. Hauchecorne, J.-P. Vigneron, J.-M. Lehn, P. Lehn, The design of cationic lipids for gene delivery., *Curr. Pharm. Des.* 11 (2005) 375–394. doi:10.2174/1381612053382133.
- [19] J. Rejman, G. Tavernier, N. Bavarsad, J. Demeester, S.C. De Smedt, mRNA transfection of cervical carcinoma and mesenchymal stem cells mediated by cationic carriers, *J. Control. Release.* 147 (2010) 385–391. doi:10.1016/j.jconrel.2010.07.124.
- [20] D. Lu, R. Benjamin, M. Kim, R.M. Conry, D.T. Curiel, Optimization of methods to achieve mRNA-mediated transfection of tumor cells in vitro and in vivo employing cationic liposome vectors., *Cancer Gene Ther.* 1 (1994) 245–52.

- [21] <https://www.thermofisher.com/order/catalog/product/LMRNA003.>, (n.d.).
- [22] C. Cheng, A.J. Convertine, P.S. Stayton, J.D. Bryers, Multifunctional triblock copolymers for intracellular messenger RNA delivery, *Biomaterials*. 33 (2012) 6868–6876. doi:10.1016/j.biomaterials.2012.06.020.
- [23] L. De Laporte, J. Cruz Rea, L.D. Shea, Design of modular non-viral gene therapy vectors, *Biomaterials*. 27 (2006) 947–954. doi:10.1016/j.biomaterials.2005.09.036.
- [24] L. Jin, X. Zeng, M. Liu, Y. Deng, N. He, Current progress in gene delivery technology based on chemical methods and nano-carriers, *Theranostics*. 4 (2014) 240–255. doi:10.7150/thno.6914.
- [25] S. Werth, B. Urban-Klein, L. Dai, S. Höbel, M. Grzelinski, U. Bakowsky, F. Czubayko, A. Aigner, A low molecular weight fraction of polyethylenimine (PEI) displays increased transfection efficiency of DNA and siRNA in fresh or lyophilized complexes, *J. Control. Release*. 112 (2006) 257–270. doi:10.1016/j.jconrel.2006.02.009.
- [26] H. Debus, P. Baumhof, J. Probst, T. Kissel, Delivery of messenger RNA using poly(ethylene imine)-poly(ethylene glycol)-copolymer blends for polyplex formation: Biophysical characterization and in vitro transfection properties, *J. Control. Release*. 148 (2010) 334–343. doi:10.1016/j.jconrel.2010.09.007.
- [27] D.S. Manickam, J. Li, D.A. Putt, Q.H. Zhou, C. Wu, L.H. Lash, D. Oupický, Effect of innate glutathione levels on activity of redox-responsive gene delivery vectors, *J. Control. Release*. 141 (2010) 77–84. doi:10.1016/j.jconrel.2009.08.022.
- [28] S. Üzgün, G. Nica, C. Pfeifer, M. Bosinco, K. Michaelis, J.F. Lutz, M. Schneider, J. Rosenecker, C. Rudolph, PEGylation improves nanoparticle formation and transfection efficiency of messenger RNA, *Pharm. Res*. 28 (2011) 2223–2232. doi:10.1007/s11095-011-0464-z.
- [29] S.Y. Lee, M.S. Huh, S. Lee, S.J. Lee, H. Chung, J.H. Park, Y.K. Oh, K. Choi, K. Kim, I.C. Kwon, Stability and cellular uptake of polymerized siRNA (poly-siRNA)/polyethylenimine (PEI) complexes for efficient gene silencing, *J. Control. Release*. 141 (2010) 339–346. doi:10.1016/j.jconrel.2009.10.007.
- [30] K. Remaut, N.N. Sanders, B.G. De Geest, K. Braeckmans, J. Demeester, S.C. De Smedt, Nucleic acid delivery: Where material sciences and bio-sciences meet, *Mater. Sci. Eng. R Reports*. 58 (2007) 117–161. doi:10.1016/j.mser.2007.06.001.
- [31] D. Ibraheem, A. Elaissari, H. Fessi, Gene therapy and DNA delivery systems, *Int. J. Pharm.* 459 (2014) 70–83. doi:10.1016/j.ijpharm.2013.11.041.
- [32] X. Xia, N. a Monteiro-Riviere, J.E. Riviere, An index for characterization of nanomaterials in biological systems, *Nat. Nanotechnol.* 5 (2010) 671–675. doi:10.1038/nnano.2010.164.
- [33] G. Maiorano, S. Sabella, B. Sorce, V. Brunetti, M.A. Malvindi, R. Cingolani, P.P. Pompa, Effects of Cell Culture Media on the Dynamic Formation of Protein-Nanoparticle Complexes and Influence on the Cellular Response, *ACS Nano*. 4 (2010) 7481–7491. doi:10.1021/nn101557e.
- [34] M. Lundqvist, J. Stigler, G. Elia, I. Lynch, T. Cedervall, K.A. Dawson, Nanoparticle size and surface properties determine the protein corona with possible implications for biological impacts, *Proc Natl Acad Sci U S A*. 105 (2008) 14265–14270. doi:10.1073/pnas.0805135105.
- [35] I. Lynch, A. Salvati, K.A. Dawson, Protein-nanoparticle interactions: What does the cell see?, *Nat. Nanotechnol.* 4 (2009) 546–7. doi:10.1038/nnano.2009.248.
- [36] D. Walczyk, F.B. Bombelli, M.P. Monopoli, I. Lynch, K.A. Dawson, What the cell ‘sees’ in bionanoscience, *J. Am. Chem. Soc.* 132 (2010) 5761–5768. doi:10.1021/ja910675v.

- [37] G.R. Dakwar, E. Zagato, J. Delanghe, S. Hobel, A. Aigner, H. Denys, K. Braeckmans, W. Ceelen, S.C. De Smedt, K. Remaut, Colloidal stability of nano-sized particles in the peritoneal fluid: Towards optimizing drug delivery systems for intraperitoneal therapy, *Acta Biomater.* 10 (2014) 2965–2975. doi:10.1016/j.actbio.2014.03.012.
- [38] H.Y. Choi, T.J. Lee, G.M. Yang, J. Oh, J. Won, J. Han, G.J. Jeong, J. Kim, J.H. Kim, B.S. Kim, S.G. Cho, Efficient mRNA delivery with graphene oxide-polyethylenimine for generation of footprint-free human induced pluripotent stem cells, *J. Control. Release.* 235 (2016) 222–235. doi:10.1016/j.jconrel.2016.06.007.
- [39] S. Bire, N. Ishac, F. Rouleux-Bonnin, In vitro synthesis, delivery, and bioavailability of exogenous mRNA in gene transfer mediated by PiggyBac transposition, *Methods Mol. Biol.* 1 (2016) 75. doi:10.1007/978-1-4939-3625-0_13.
- [40] M. Zhao, M. Li, Z. Zhang, T. Gong, X. Sun, Induction of HIV-1 gag specific immune responses by cationic micelles mediated delivery of gag mRNA, *Drug Deliv.* 7 (2015) 2596–2607. doi:10.3109/10717544.2015.1038856.
- [41] K. Buyens, B. Lucas, K. Raemdonck, K. Braeckmans, J. Vercammen, J. Hendrix, Y. Engelborghs, S.C. De Smedt, N.N. Sanders, A fast and sensitive method for measuring the integrity of siRNA-carrier complexes in full human serum, *J. Control. Release.* 126 (2008) 67–76. doi:10.1016/j.jconrel.2007.10.024.
- [42] K. Remaut, B. Lucas, K. Braeckmans, N.N. Sanders, S.C. De Smedt, J. Demeester, FRET-FCS as a tool to evaluate the stability of oligonucleotide drugs after intracellular delivery, *J. Control. Release.* 103 (2005) 259–271. doi:10.1016/j.jconrel.2004.11.019.
- [43] K. Remaut, B. Lucas, K. Braeckmans, N.N. Sanders, J. Demeester, S.C. De Smedt, Delivery of Phosphodiester Oligonucleotides: Can DOTAP/DOPE Liposomes Do the Trick?, *Biochemistry.* 45 (2006) 1755–1764. doi:10.1021/bi0519755.
- [44] D. Magde, E. Elson, W.W. Webb, Thermodynamic fluctuations in a reacting system measurement by fluorescence correlation spectroscopy, *Phys. Rev. Lett.* 29 (1972) 705–708. doi:10.1103/PhysRevLett.29.705.
- [45] G. Bonnet, O. Krichevsky, Fluorescence correlation spectroscopy: the technique and its applications, *Reports Prog. Phys.* 65 (2002) 251–297. doi:10.1088/0034-4885/65/2/203.
- [46] E.L. Elson, Fluorescence correlation spectroscopy: Past, present, future, *Biophys. J.* 101 (2011) 2855–2870. doi:10.1016/j.bpj.2011.11.012.
- [47] B. Lucas, K. Remaut, N.N. Sanders, K. Braeckmans, S.C. De Smedt, J. Demeester, Towards a better understanding of the dissociation behavior of liposome-oligonucleotide complexes in the cytosol of cells, *J. Control. Release.* 103 (2005) 435–450. doi:10.1016/j.jconrel.2004.12.017.
- [48] K. Rombouts, T.F. Martens, E. Zagato, J. Demeester, S.C. De Smedt, K. Braeckmans, K. Remaut, Effect of covalent fluorescence labeling of plasmid DNA on its intracellular processing and transfection with lipid-based carriers, *Mol. Pharm.* 11 (2014) 1359–1368. doi:10.1021/mp4003078.
- [49] K. Remaut, B. Lucas, K. Raemdonck, K. Braeckmans, J. Demeester, S.C. De Smedt, Can we better understand the intracellular behavior of DNA nanoparticles by fluorescence correlation spectroscopy?, *J. Control. Release.* 121 (2007) 49–63. doi:10.1016/j.jconrel.2007.04.008.
- [50] K. Remaut, B. Lucas, K. Braeckmans, N.N. Sanders, J. Demeester, S.C. De Smedt, Protection of oligonucleotides against nucleases by pegylated and non-pegylated liposomes as studied by

- fluorescence correlation spectroscopy, *Biomacromolecules*. 8 (2007) 1333–1340. doi:10.1016/j.jconrel.2005.09.048.
- [51] W. Li, F.C. Szoka, Lipid-based Nanoparticles for Nucleic Acid Delivery, *Pharm. Res.* 24 (2007) 438–449. doi:10.1007/s11095-006-9180-5.
- [52] A. El Ouahabi, V. Pector, R. Fuks, M. Vandenbranden, J.M. Ruyschaert, Double long-chain amidine liposome-mediated self replicating RNA transfection, *FEBS Lett.* 380 (1996) 108–112. doi:10.1016/0014-5793(96)00038-5.
- [53] C.L. Gebhart, A. V Kabanov, Evaluation of polyplexes as gene transfer agents, *J. Control. Release.* 73 (2001) 401–416. www.elsevier.com (accessed 24 October 2017).
- [54] K. Kunath, A. Von Harpe, D. Fischer, H. Petersen, U. Bickel, K. Voigt, T. Kissel, Low-molecular-weight polyethylenimine as a non-viral vector for DNA delivery: comparison of physicochemical properties, transfection efficiency and in vivo distribution with high-molecular-weight polyethylenimine, *J. Control. Release.* 89 (2003) 113–125. www.elsevier.com (accessed 24 October 2017).
- [55] D. Fischer, R. Bhattacharya, B. Osburg, U. Bickel, Inhibition of monocyte adhesion on brain-derived endothelial cells by NF-kappaB decoy/polyethylenimine complexes, *J. Gene Med.* 7 (2005) 1063–1076. doi:10.1002/jgm.747.
- [56] O. Boussif, F. Lezoualc'ht, M. Antonietra Zanta, D. Mergny, D. Schermant, B. Demeneix, J.-P. Behr, A versatile vector for gene and oligonucleotide transfer into cells in culture and in vivo: Polyethylenimine, *Biochemistry.* 92 (1995) 7297–7301.
- [57] A. Elouahabi, R. Jean-Marie, Formation and Intracellular Trafficking of Lipoplexes and Polyplexes, *Mol. Ther.* 11 (2005) 336–347. doi:org/10.1016/j.ymthe.2004.12.006.
- [58] M. Ogris, P. Steinlein, S. Carotta, S. Brunner, E. Wagner, DNA/polyethylenimine transfection particles: Influence of ligands, polymer size, and PEGylation on internalization and gene expression, *AAPS PharmSci.* 3 (2001) 43–53. doi:10.1208/ps030321.
- [59] T. Bieber, W. Meissner, S. Kostin, A. Niemann, H.-P. Elsasser, Intracellular route and transcriptional competence of polyethylenimine-DNA complexes, *J. Control. Release.* 82 (2002) 441–454. doi:org/10.1016/S0168-3659(02)00129-3.
- [60] M.L. Read, K.H. Bremner, D. Oupický, N.K. Green, P.F. Searle, L.W. Seymour, Vectors based on reducible polycations facilitate intracellular release of nucleic acids, *J. Gene Med.* 5 (2003) 232–245. doi:10.1002/jgm.331.
- [61] Y.L. Jang, S.H. Ku, S.J. Lee, J.H. Park, W.J. Kim, I.C. Kwon, S.H. Kim, J.H. Jeong, Hyaluronic Acid-siRNA Conjugate/Reducible Polyethylenimine Complexes for Targeted siRNA Delivery, *J. Nanosci. Nanotechnol.* 14 (2014) 7388–7394. doi:10.1166/jnn.2014.9583.
- [62] K. Paunovska, C.D. Sago, C.M. Monaco, W.H. Hudson, M.G. Castro, T.G. Rudoltz, S. Kalathoor, D.A. Vanover, P.J. Santangelo, R. Ahmed, A. V Bryksin, J.E. Dahlman, W.H. Coulter, A Direct Comparison of in Vitro and in Vivo Nucleic Acid Delivery Mediated by Hundreds of Nanoparticles Reveals a Weak Correlation, *Nano Lett.* 18 (2018) 2148–2157. doi:10.1021/acs.nanolett.8b00432.
- [63] B. Lucas, K. Remaut, N.N. Sanders, K. Braeckmans, S.C. De Smedt, J. Demeester, Studying the Intracellular Dissociation of Polymer-Oligonucleotide Complexes by Dual Color Fluorescence Fluctuation Spectroscopy and Confocal Imaging, *Biochemistry.* 44 (2005) 9905–9912. doi:10.1021/bi0476883.

Figures:

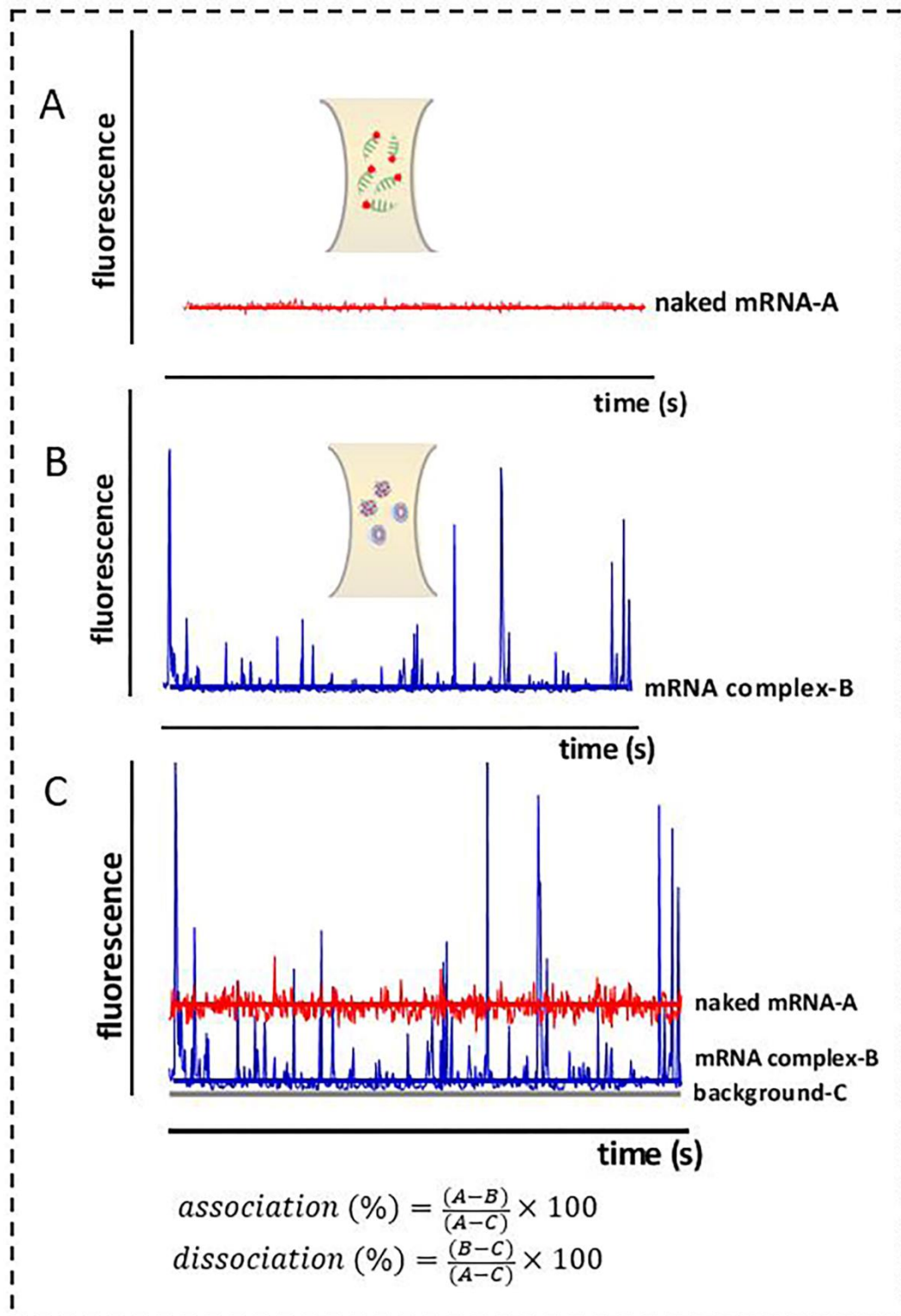


Figure 1. (A) Fluorescence fluctuations of naked Cy5 labeled mRNA recorded by FCS in function of time. (B) Fluorescence profile of mRNA-lipoplexes or mRNA-polyplexes measured by FCS. The high fluorescence peaks are the complexes containing multiple fluorescent mRNA molecules, while the fluorescence signal between peaks is the naked fluorescent mRNA. (C) Calculation of association/dissociation degree (%) of mRNA complexes.

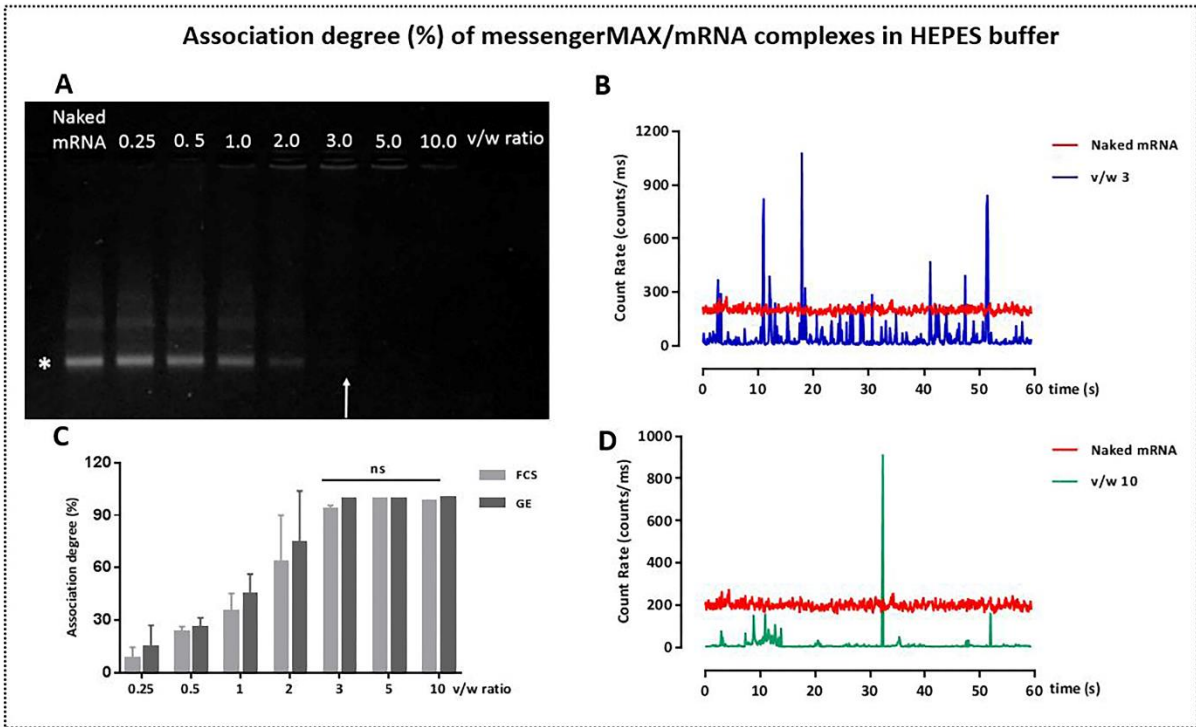


Figure 2. Association degree (%) of messengerMAX/mRNA, prepared at different v/w ratios, in HEPES buffer. (A) Representative gel for naked and complexed mRNA with v/w ratios as depicted above the gel. The star indicates the level of naked mRNA in the gel, while the arrow shows the v/w ratio from which full complexation starts. (B, D) Representative fluorescence fluctuations as measured with FCS for naked mRNA (red) and messengerMAX/mRNA complexes with v/w ratio 3 (blue) and 10 (green) respectively. (C) shows the association degree (%) calculated from 3 independent FCS (gray bars) and gel (dark gray bars) measurements.

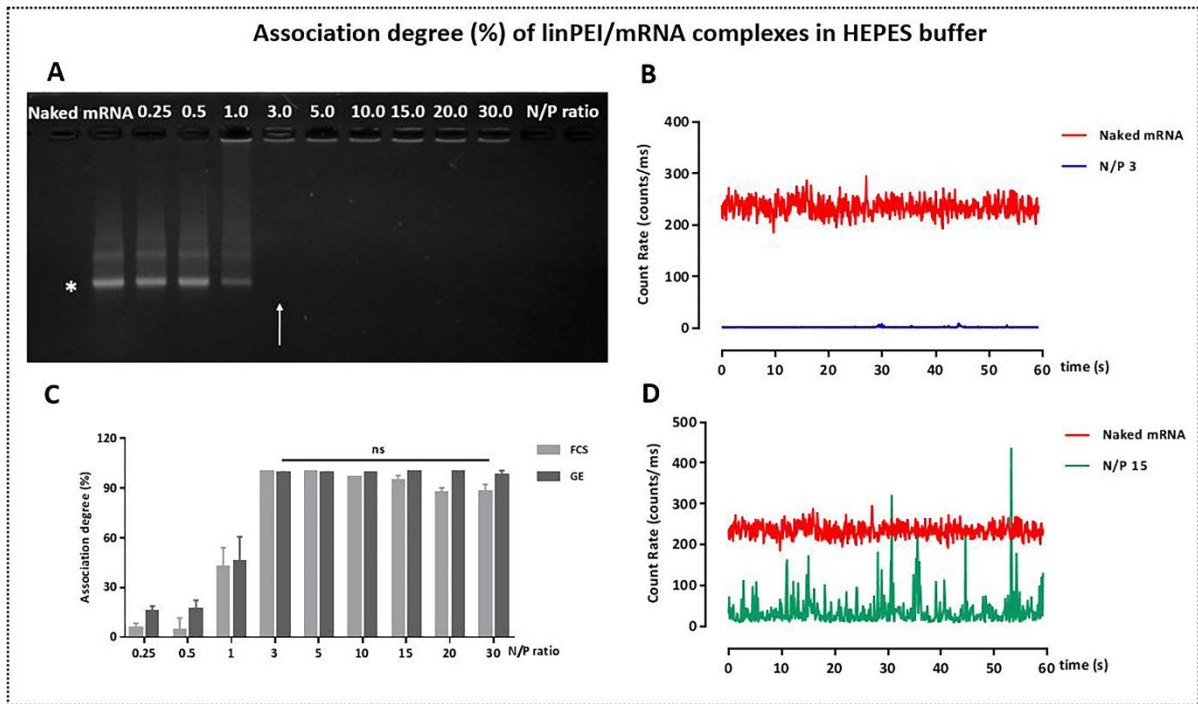


Figure 3. Association degree (%) of linPEI/mRNA, prepared at different N/P ratios, in HEPES buffer. (A) Representative gel for naked and complexed mRNA with N/P ratios as depicted above the gel. The star indicates the level of naked mRNA in the gel, while the arrow shows the N/P ratio from which full complexation starts. (B, D) Representative fluorescence fluctuations as measured with FCS for naked mRNA (red) and linPEI/mRNA complexes with N/P ratio 3 (blue) and 15 (green) respectively. (C) shows the association degree (%) calculated from 3 independent FCS (gray bars) and gel (dark gray bars) measurements.

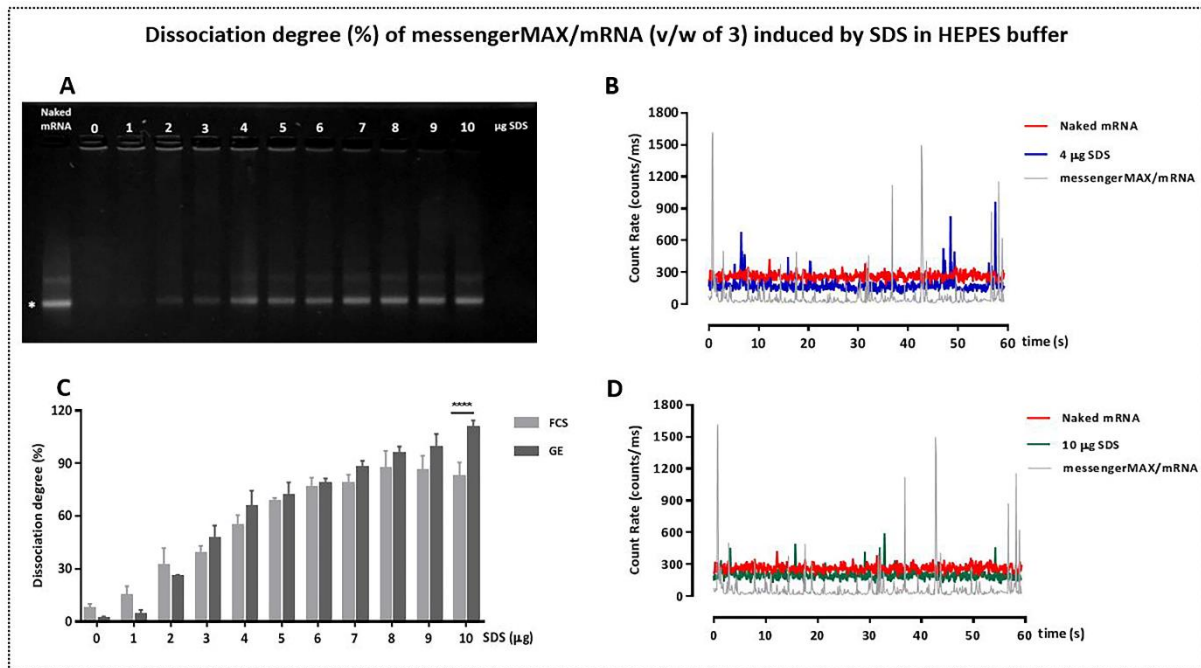


Figure 4. Dissociation degree (%) of messengerMAX/mRNA (v/w ratio 3) induced by SDS in HEPES buffer. (A) Representative gel for naked and complexed mRNA with increasing amounts of SDS as depicted above the gel. The star indicates the level of naked mRNA in the gel. (B, D) Representative fluorescence fluctuations as measured with FCS for naked mRNA (red) and messengerMAX/mRNA complexes before (grey) and after addition of 4 µg SDS (blue) and 10 µg SDS (green) respectively. (C) shows the association degree (%) calculated from 3 independent FCS (gray bars) and gel (dark gray bars) measurements. ($P < 0.0001$, ****)

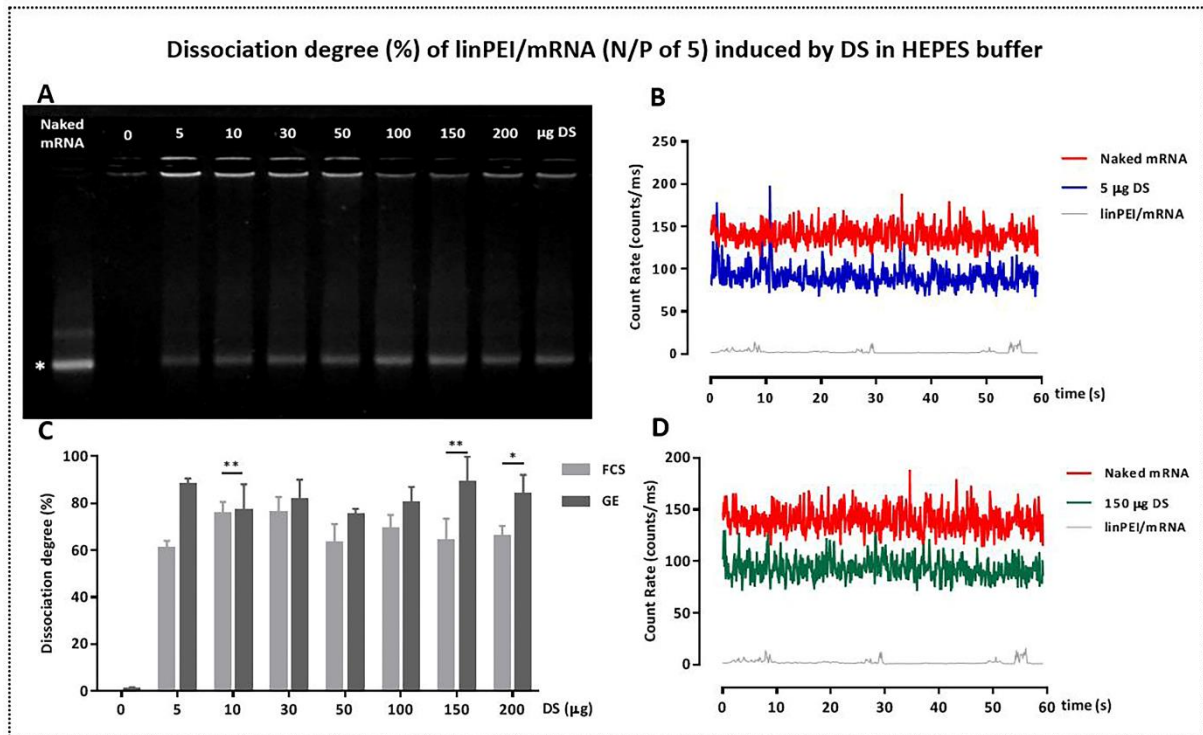


Figure 5. Dissociation degree (%) of linPEI/mRNA (N/P ratio 5) induced by DS in HEPES buffer. (A) Representative gel for naked and complexed mRNA with increasing amounts of DS as depicted above the gel. The star indicates the level of naked mRNA in the gel. (B, D) Representative fluorescence fluctuations as measured with FCS for naked mRNA (red) and linPEI/mRNA complexes before (grey) and after addition of 5 µg DS (blue) and 150 µg DS (green) respectively. (C) shows the association degree calculated from 3 independent FCS (gray bars) and gel (dark gray bars) measurements. ($P < 0.05$, *; $P < 0.001$, **)

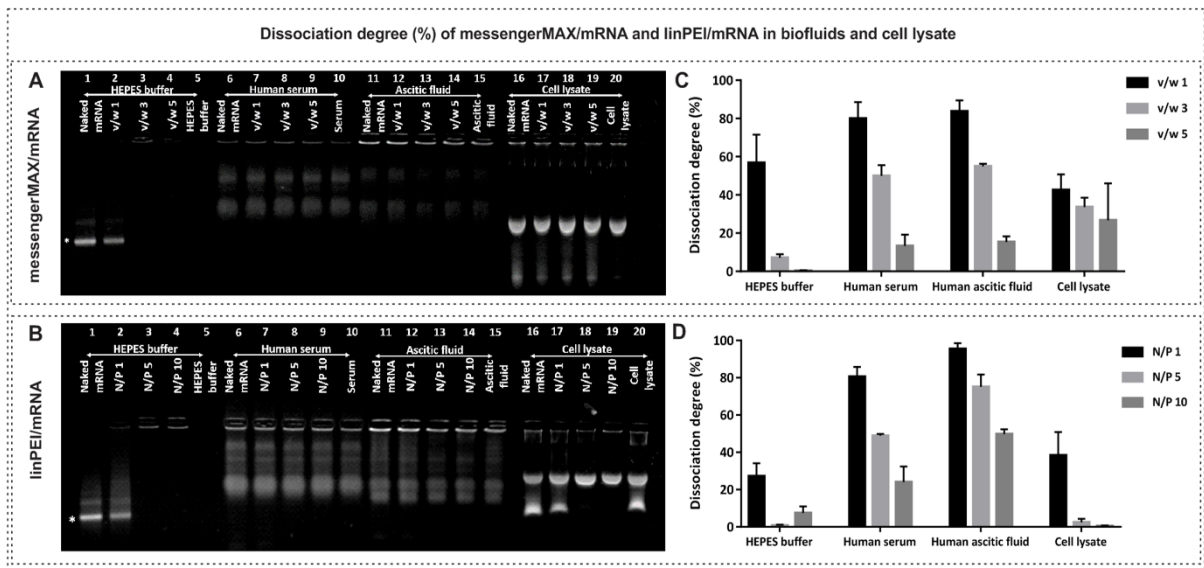


Figure 6. Stability of messengerMAX/mRNA with v/w ratio of 1 (black bars), 3 (gray bars) and 5 (dark gray bars) and linPEI/mRNA with N/P ratio of 1 (black bars), 5 (gray bars) and 10 (dark gray bars) in HEPES buffer, 80 vol% biological fluids (human serum and human ascitic fluid) and 80 vol% cell lysate after incubation at 37°C for 1 h by 1% agarose gel electrophoresis (A, B) and corresponding dissociation degree (%) as calculated from three independent FCS measurements (C, D). The star indicates the level of naked mRNA in HEPES buffer in the gel.

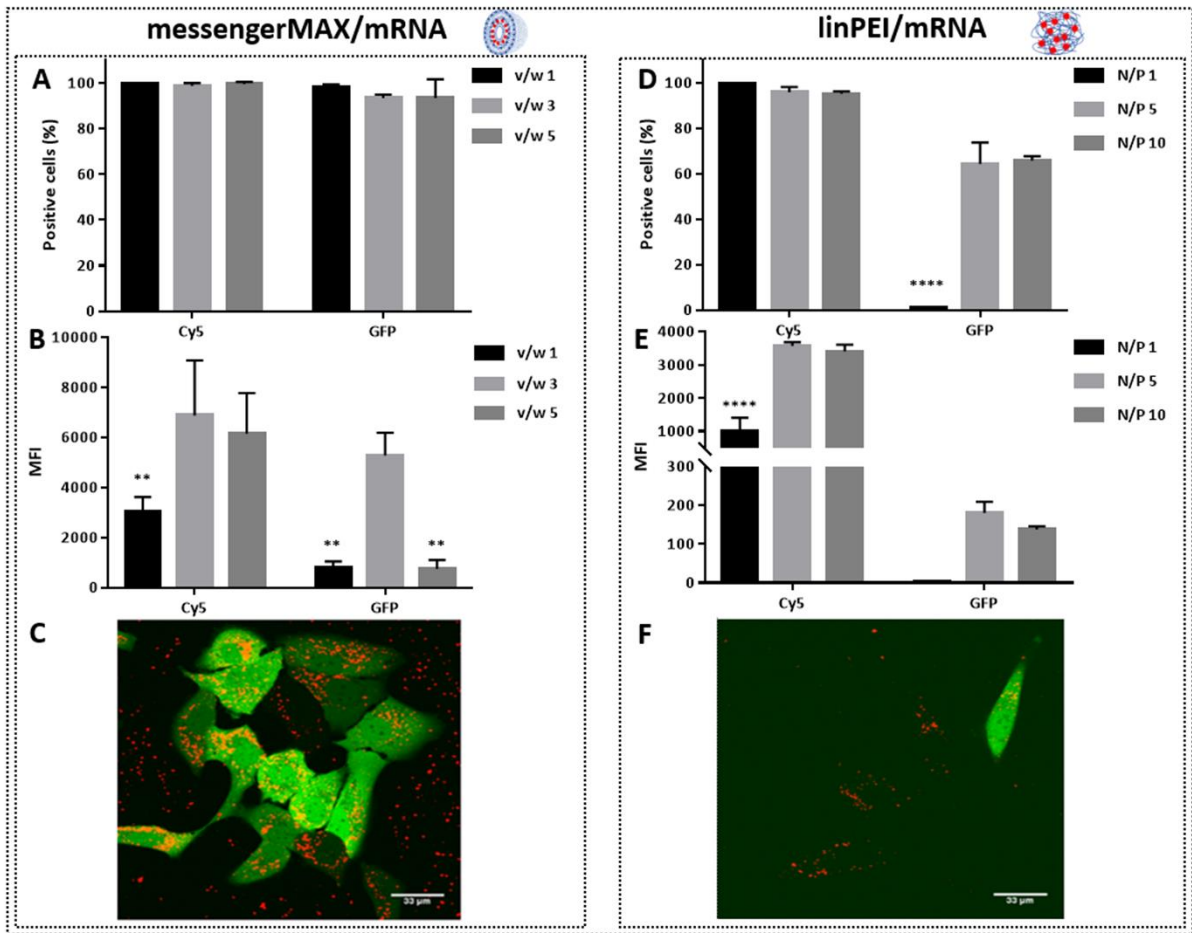


Figure 7. Uptake and transfection efficiency of (A-C) messengerMAX/mRNA with v/w ratio 1 (black bars), 3 (gray bars) and 5 (dark gray bars) and (D-F) linPEI/mRNA with N/P ratio 1 (black bars), 5 (gray bars) and 10 (dark gray bars) after incubation in Opti-MEM for 1 h. (A, D) Percentage of Cy5 and GFP positive cells after 4 h and 24 h incubation at 37°C, respectively. (B, E) MFI of Cy5 and GFP positive cells after 4 h and 24 h incubation at 37°C, respectively. All the data are averaged from 3 independent flow cytometry measurements. Images of SKOV-3 cells transfected with (C) messengerMAX/mRNA (v/w of 3) and (F) linPEI/mRNA (N/P of 5) after incubation in Opti-MEM at 37°C for 24 h. Cy5: red fluorescence; GFP: green fluorescence. Scale bar: 33 μ m.

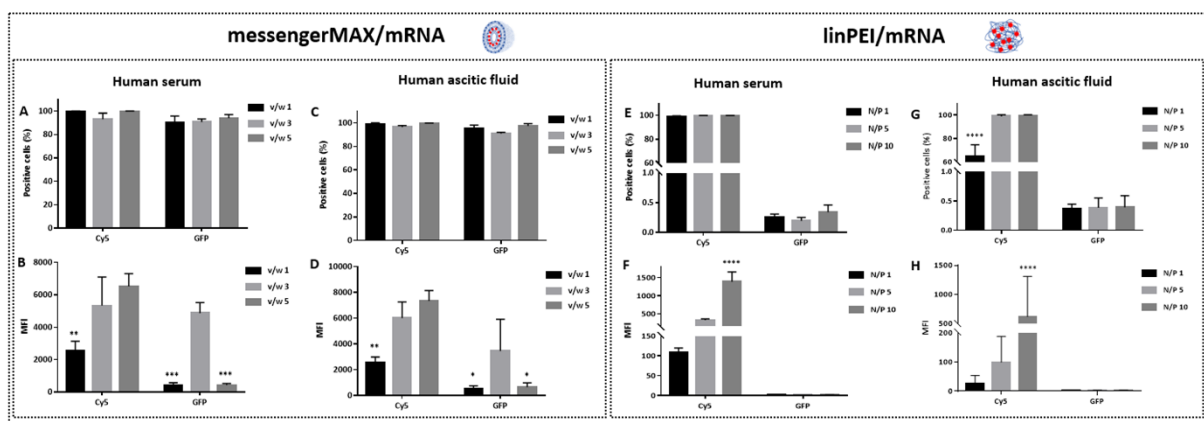
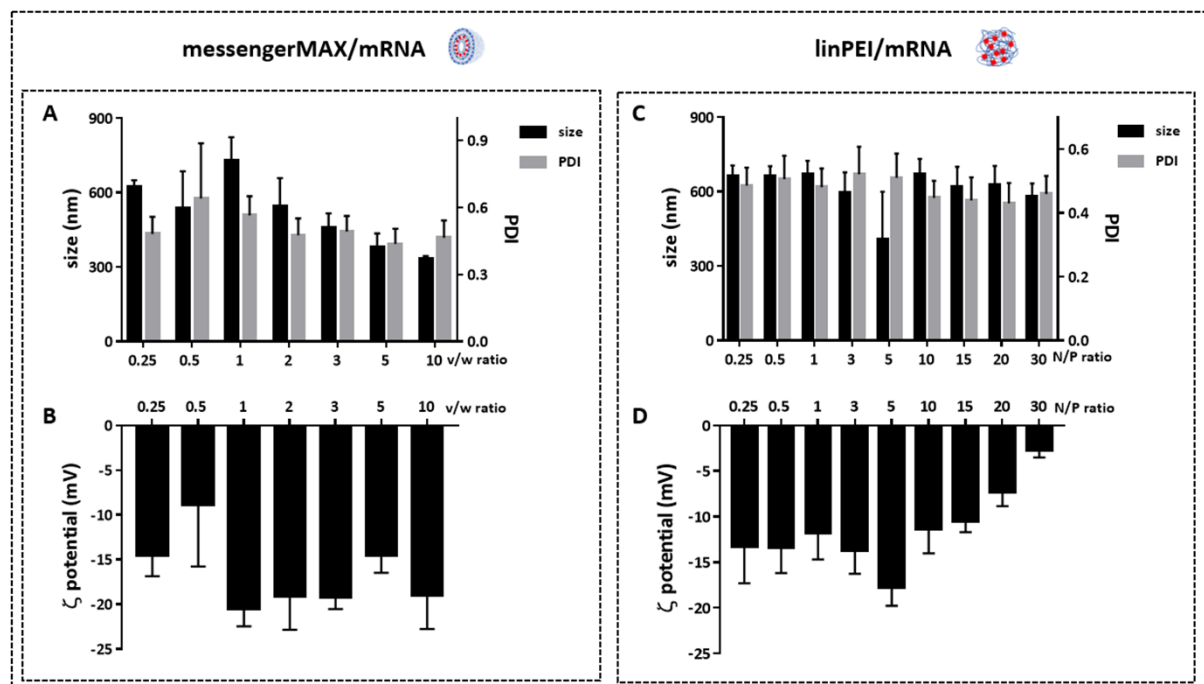
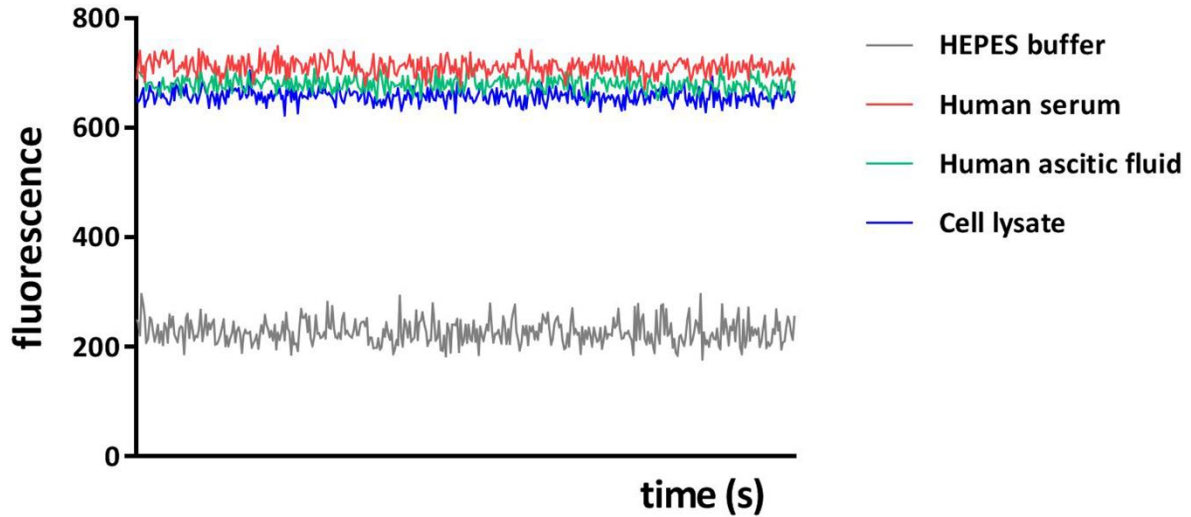


Figure 8. Uptake and transfection efficiency of (A-D) messengerMAX/mRNA with v/w ratio 1 (black bars), 3 (gray bars) and 5 (dark gray bars) and (E-H) linPEI/mRNA with N/P ratio 1 (black bars), 5 (gray bars) and 10 (dark gray bars) after incubation in human serum and human ascitic fluid for 1 h at 37°C. (A, C, E, G) Percentage and (B, D, F, H) MFI of Cy5 positive cells (after 4 h incubation at 37°C) and GFP expressing cells (after 24 h incubation at 37°C). All the data are averaged from 3 independent flow cytometry measurements.

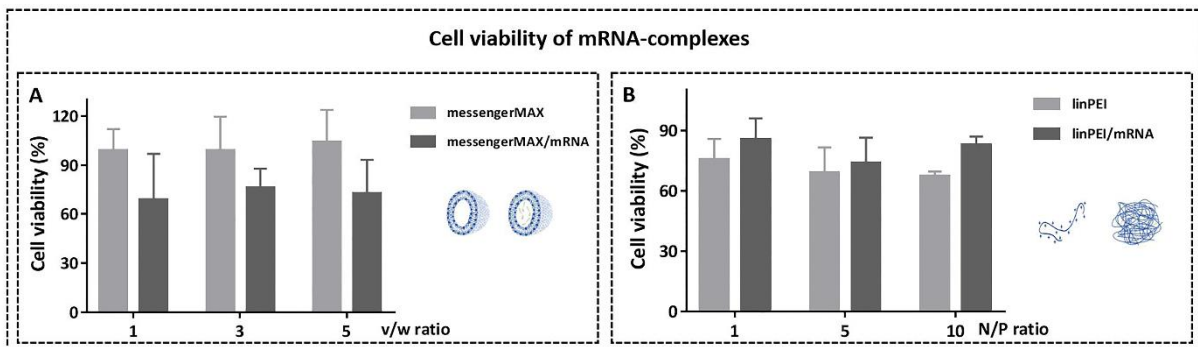
Supplementary figures



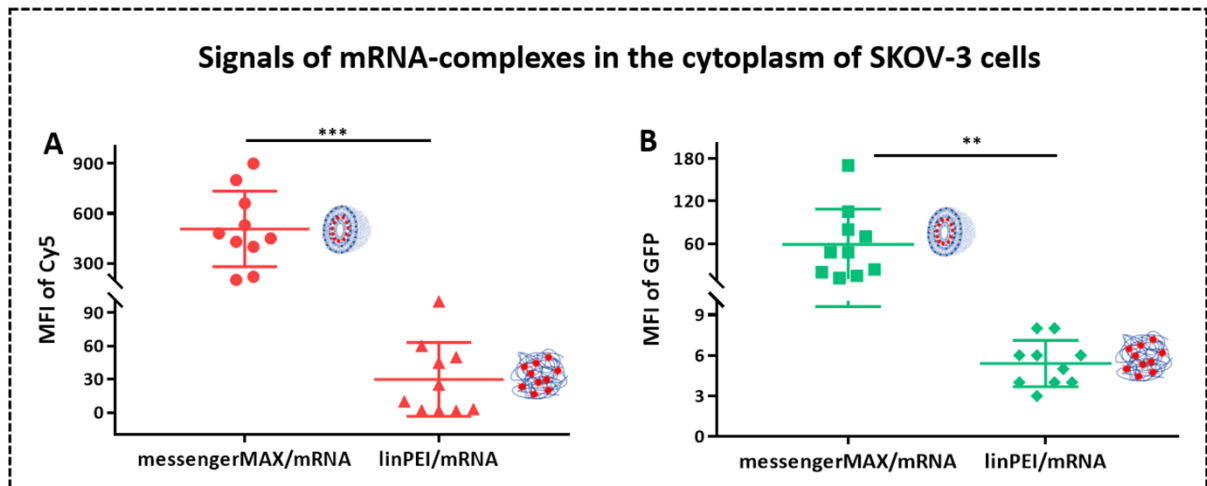
Supplementary Figure 1. Characteristics of (A, B) messengerMAX/mRNA with varying v/w ratios (C, D) linPEI/mRNA with varying N/P ratios in HEPES buffer. All the data are averaged from 3 independent DLS measurements.



Supplementary Figure 2. Fluorescence fluctuations of Cy5-mRNA recorded by FCS, after incubation in HEPES buffer (gray), undiluted human serum (red), undiluted ascitic fluid (green) and cell lysate (blue) at 37°C for 1 h. Mean fluorescence of Cy5 in human serum, ascitic fluid and cell lysate was around 3 times that of HEPES buffer, due to the degradation of mRNA observed on gel (Figure 6A and 6B).



Supplementary Figure 3. Cell viability of (A) messengerMAX (gray bars) and messengerMAX/mRNA (dark gray bars) with v/w ratio 1, 3 and 5 and (B) linPEI (gray bars) and linPEI/mRNA (dark gray bars) with N/P ratio 1, 5 and 10 after incubation in Opti-MEM for 4 h at 37°C. To avoid interference of fluorescence from Cy5 with the MTT read-out, non-labeled mRNA with exactly the same modification was complexed into lipoplexes and polyplexes. All the data are averaged from 3 independent measurements.



Supplementary Figure 4. Mean fluorescence intensity of (A) Cy5 and (B) GFP as detected by FCS in the cytoplasm of SKOV-3 cells after 4 h incubation with messengerMAX/mRNA (v/w 3) and linPEI/mRNA (N/P 5) in Opti-MEM at 37°C. All the data are averaged from 3 independent FCS measurements.